AMERICAN SOCIETY FOR MICROBIOLOGY | Microbiology Spectrum

| Virology | Research Article

Potent small molecule inhibitors against the 3C protease of foot-and-mouth disease virus

Yunjeong Kim,[1] Emma Pool,[1] Eunji Kim,[1] Chamandi S. Dampalla,[2] Harry Nhat Nguyen,[2] David K. Johnson,[3] Scott Lovell,[4] William C. Groutas,[2] Kyeong-Ok Chang[1]

AUTHOR AFFILIATIONS See affiliation list on p. 13.

ABSTRACT Foot-and-mouth disease (FMD) is one of the most devastating diseases of livestock which can cause significant economic losses, especially when introduced to FMD-free countries. FMD virus (FMDV) belongs to the family *Picornaviridae* and is antigenically heterogeneous with seven established serotypes. The prevailing preventive and control strategies are limited to restriction of animal movement and elimination of infected or exposed animals, which can be potentially combined with vaccination. However, FMD vaccination has limitations including delayed protection and lack of cross-protection against different serotypes. Recently, antiviral drug use for FMD outbreaks has increasingly been recognized as a potential tool to augment the existing early response strategies, but limited research has been reported on potential antiviral compounds for FMDV. FMDV 3C protease (3Cpro) cleaves the viral-encoded polyprotein into mature and functional proteins during viral replication. The essential role of viral 3Cpro in viral replication and the high conservation of 3Cpro among different FMDV serotypes make it an excellent target for antiviral drug development. We have previously reported multiple series of inhibitors against picornavirus 3Cpro or 3C-like proteases (3CLpros) encoded by coronaviruses or caliciviruses. In this study, we conducted structure-activity relationship studies for our in-house focused compound library containing 3Cpro or 3CLpro inhibitors against FMDV 3Cpro using enzyme and cell-based assays. Herein, we report the discovery of aldehyde and α-ketoamide inhibitors of FMDV 3Cpro with high potency. These data inform future preclinical studies that are related to the advancement of these compounds further along the drug development pathway.

IMPORTANCE Food-and-mouth disease (FMD) virus (FMDV) causes devastating disease in cloven-hoofed animals with a significant economic impact. Emergency response to FMD outbreaks to limit FMD spread is critical, and the use of antivirals may overcome the limitations of existing control measures by providing immediate protection for susceptible animals. FMDV encodes 3C protease (3Cpro), which is essential for virus replication and an attractive target for antiviral drug discovery. Here, we report a structure-activity relationship study on multiple series of protease inhibitors and identified potent inhibitors of FMDV 3Cpro. Our results suggest that these compounds have the potential for further development as FMD antivirals.

KEYWORDS food-and-mouth disease, 3C protease, protease inhibitor, antiviral, structure-activity relationships

Foot-and-mouth disease (FMD) is a highly contagious disease affecting cloven-hoofed animals and one of the most devastating diseases with a significant economic impact. The classic signs of FMD in cattle and pigs include fever and vesicular lesions on the feet, mouth, and mammary glands, which result in severe production losses

Editor Luis M. Schang, Cornell University College of Veterinary Medicine, Ithaca, USA

Address correspondence to Yunjeong Kim, ykim@ksu.edu, or Kyeong-Ok Chang, kchang@vet.ksu.edu.

Y.K., W.G., and K.C. have patents or patent pending for the compound series. All other authors declare no potential conflict of interest.

See the funding table on p. 13.

Received 14 September 2023
Accepted 18 January 2024
Published 11 March 2024

(reviewed in reference 1). Foot-and-mouth disease virus (FMDV) is a single-stranded, positive-sense RNA virus and belongs to the *Aphthovirus* genus within the family *Picornaviridae*. FMDV is antigenically heterogeneous, and seven serotypes are recognized worldwide: O, A, C, Asia1, Southern African Territories 1 (SAT), SAT2, and SAT3 (2). Furthermore, there is considerable antigenic diversity within each serotype with over 60 subtypes (1, 2). FMD is endemic in several parts of Asia and throughout most of Africa and the Middle East (2), but outbreaks sporadically occur in non-endemic areas and countries as FMDV is easily spread by aerosols and contact with contaminated materials and infected animals and animal products (1, 2). The United States has been FMD free without vaccination since 1929. However, there is a continuing risk of FMD transmission into the U.S. soil through international trades of animal and animal products (3). FMD outbreaks in the United States would have a catastrophic impact on the economy extending far beyond animal agriculture, and it is estimated that the impacts of FMD outbreaks in the United States would cost several to hundreds of billion dollars (4–6).

Effective control of FMD outbreaks requires rapid response due to a wide range of susceptible animals and the highly contagious nature of FMDV. Therefore, early detection, quarantine, and movement control are critical activities to limit FMD spread. Traditional FMD response strategies involve stamping out, which is depopulation of infected and in-contact susceptible animals, as an integral component, which can be combined with vaccination with or without subsequent depopulation of vaccinated animals depending on epidemiologic considerations (4). In countries that are free from FMD without vaccination, such as the US, stamping-out strategy alone may not sufficiently control FMD outbreaks, especially in densely populated areas, which may require FMD emergency vaccination (6). However, there are many challenges related to FMD emergency vaccination including delayed onset of protection, little or no cross-protection across serotypes and subtypes, and limitation of export from the loss of FMD-free without vaccination status. Therefore, antiviral agents are increasingly recognized as a potential measure, as supplemental or alternative to vaccination, to enhance emergency response system (7, 8).

Some direct-acting antivirals targeting viral polymerase RNA and viral RNA (RNA interference) and interferon or interferon-inducing agents against FMDV have been reported (9–24). However, only limited research is available on protease inhibitors that target FMDV (25–27). FMDV 3C protease (3Cpro) cleaves the viral polyprotein into mature, functional proteins during viral replication. The essential role of virus protease in replication and the high conservation of 3Cpro among different FMDV serotypes make it an excellent target for antiviral drug development. We have previously reported multiple series of protease inhibitors for important human and animal viruses that encode 3Cpro or 3C-like protease (3CLpro) (28–46). In this study, we conducted structure-activity relationship studies using our in-house focused compound library with the fluorescence resonance energy transfer (FRET) assay (35) and cell-based reporter assay for FMDV 3Cpro and identified potent aldehyde and α-ketoamide inhibitors. The identified inhibitors are well suited to conducting further preclinical studies to evaluate their potential as drug candidates. Furthermore, homology modeling and docking studies were conducted to illuminate the structural basis for the observed potency of the FMD 3Cpro inhibitors.

MATERIALS AND METHODS

Multiple sequence alignment of 3Cpro of FMDV strains

The 3Cpro sequences of 18 FMDV prototypes belonging to seven major serotypes (O, A, C, Asia 1, SAT 1–3) were obtained from the GenBank. The FMDV strains were A/IND287/96 (GenBank accession no. ACJ02492), O1/BFS 1860/UK/67 (AY593815), O1/Manisa/TUR/69 (AY593823), A21/Lumbwa/KEN/3/64 (AY593761), A22/IRQ/24/64 (AY593763), C/UK/149/34 (AY593810), C1/Santa Pau/Spain/70 (AJ133357), Asia1/PAK/1/54 (AY593795), Asia1/IND/63/72 (AY304994), Asia1/

YNBS/China/58 (AY390432), SAT1/RV/11/37 (AY593839), SAT1/BEC/1/48 (AY593838), SAT1/ISR/4/62 (AY593844), SAT2/SA/106/59 (AY593848), SAT2/ZIM/7/83 (AF540910), SAT2/RHO/1/48 (AY593847), SAT3/SA/57/59 (AY593850), and SAT3/BEC/1/65 (AY593853). The FMDV 3Cpro amino acid sequences were aligned using Clustal Omega (https://www.ebi.ac.uk/Tools/msa/clustalo/) to determine amino acid homology.

Compounds

The compounds included in this study are listed in Tables 1 to 3. Syntheses of these compounds were published elsewhere (38, 40, 45, 47). AG7088 (Rupintrivir) was purchased from MedChemExpress, LLC (Monmouth Junction, NJ).

The FRET assay

Expression of recombinant FMDV 3Cpro

To express recombinant FMDV 3Cpro, the full sequence of 3Cpro of A/IND287/96 strain (GenBank accession no. ACJ02492, serotype A) encoding 213 amino acids and N-terminal 6 His tags was codon optimized for protein expression in *E. coli* and synthesized by Integrated DNA Technologies (Coralville, IA). The synthesized DNA was cloned into pET-28a(+) vector (Addgene, Cambridge, MA), and the recombinant 3Cpro was expressed in *E. coli* BL21 cells (Invitrogen, Carlsbad, CA) grown in Luria-Bertani broth by induction with 1 mM isopropyl β-D-thiogalactopyranoside. The recombinant proteins of 16.5 kDa were then purified using HIS Gravitrap Ni-NTA affinity columns (GE Healthcare, Chicago, IL) following the standard protocol (35).

Activity of FMDV 3Cpro and inhibition assay

To confirm the activity of 3Cpro, the expressed 3Cpro was serially diluted in assay buffer (50 mM NaCl, 6 mM dithiothreitol, 50 mM HEPES, 0.4 mM EDTA, and 60% glycerol at pH 8.0) and mixed with FRET substrate, Edans-APAKQLLN-Dabcyl (AnaSpec, Fremont, CA), and the mixture was added into a black 96-well microplate (Fisher Scientific, Waltham, MA). The plate was then measured for fluorescence at excitation and emission values 360 and 460 nm, respectively, on a fluorescence microplate reader (FLx800, Biotek, Winnooski, VT) for up to 90 min. After the activity of the expressed 3Cpro was confirmed, potency of the compounds was determined against FMDV 3Cpro, as previously described by us (35, 48). Briefly, each compound was serially diluted in DMSO or media and incubated with FMDV 3Cpro in assay buffer at room temperature (RT) for 30 min. Then, the FRET substrate was added to the mixture in a black 96-well microplate. Following incubation of the plate at RT for 30 min, fluorescence was measured on the microplate reader, and the relative fluorescence was calculated by subtracting the values for substrate-only control from the raw values. The 50% inhibitory concentration (IC_{50}) was calculated using the non-linear regression analysis with four parameter variable slope in GraphPad Prism software version 9 (GraphPad Software, La Jolla, CA), as previously described (35, 48).

Cell-based reporter assay

Generation of plasmids encoding the FMDV 3Cpro and circular, permutated form of firefly luciferase

The full-length 3Cpro of FMDV A/IND287/96 strain was codon optimized for protein expression in mammalian cells and synthesized by Integrated DNA Technologies. The gene was then cloned into pcDNA3 H2B-mIFP T2A vector (Addgene, Watertown, MA). The resulting plasmid was designated as pcDNA3-FMDV-3Cpro. The pGloSensor-30F-DEVDG plasmid encodes a circular, permutated form of firefly luciferase gene containing a caspase 3/7 cleavage site sequence and was obtained from Promega (Madison, WI) (49). The cleavage sequence was swapped with an FMDV 3Cpro cleavage sequence (APAKQLLN) using a QuikChange II Site-directed mutagenesis kit (Agilent, Santa Clara,

TABLE 1 The IC_{50}, EC_{50}, and CC_{50} values of dipeptidyl (α-ketoamide or heterocycle compounds ***E6a–E8a*** [37] and tripeptidyl compounds ***E1*** [**NPI52**] and *E6* [38]) against FMDV 3Cpro in the FRET and cell-based reporter assays

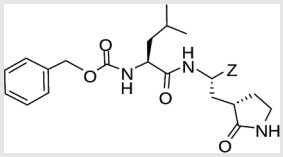

Compound	Z	FRET assay (IC_{50}, μM)[a]	Cell-based assay (EC_{50}, μM)[b]	CC_{50} (μM)
GC373		2.3 ± 0.07[c]	6.6 ± 0.2	>50
E6a		3.9 ± 0.2	NT[d]	>50
E6b		2.4 ± 0.09	8.8 ± 0.3	>50
E6c		2.1 ± 0.07	7.0 ± 0.5	>50
E6d	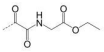	2.2 ± 0.05	9.2 ± 0.1	>50
E6e		2.8 ± 0.1	NT	>50
E6g		1.5 ± 0.1	5.8 ± 0.3	>50
E8a		3.4 ± 0.08	8.2 ± 0.09	>50
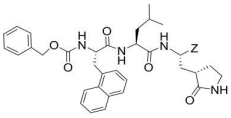				
E 1 (NPI52)		0.05 ± 0.08	0.11 ± 0.05	>50
E6		0.06 ± 0.06	0.15 ± 0.07	>50
AG7088	NA	4.3 ± 0.2	10.3 ± 0.2	>50

[a]IC_{50}, 50% inhibitory concentration.
[b]EC_{50}, 50% effective concentration; CC_{50}, 50% cytotoxic concentration (values are M ± SD).
[c]Mean (M) ± standard deviation (SD) of the means.
[d]NT, not tested.

CA), and the resulting plasmid was designated as pGlo-FMDV. The pGloSensor-30F plasmid contains Renilla luciferase gene as an expression control

Cell-based reporter assay

Trypsinized HEK293T cells were electroporated with pGlo-FMDV and pcDNA3-FMDV-3Cpro (10 ng of each plasmid) using a Neon Electroporation system (Thermo Fisher, Chicago, IL). Electroporation of pGlo-FMDV alone resulted in minimal background luminescence at 24 h after electroporation. After electroporation, cells were incubated with DMSO (0.1%) or each compound at 10, 2, 0.5, 0.1, and 0.02 μM for 20 h. Following lysis of the cells, firefly and Renilla luciferases were measured using a dual luciferase reporter assay (Promega, Madison, WI) on a luminometer (GloMax 20/20 Luminometer, Promega), following the manufacturer's direction. Firefly luciferase was normalized against Renilla luciferase, and the 50% effective concentration (EC_{50}) of each compound was calculated by GraphPad Prism software. Figure 1B illustrates the cell-based reporter assay.

TABLE 2 The IC_{50}, EC_{50}, and CC_{50} values of cyclopropane-based compounds (***C1c/d-C17c/d*** [40]) against FMDV 3Cpro in the enzyme and cell-based report assays

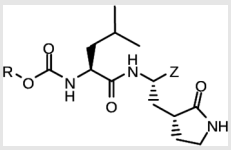

Compound	R	Z	FRET assay (IC_{50}, μM)[a]	Cell-based assay (EC_{50} μM)[b]	CC_{50} (μM)
C1c	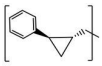	-CHO	1.00 ± 0.28[c]	3.15 ± 0.35	>50
C1d		-CH(OH)SO_3Na	0.75 ± 0.07	3.25 ± 0.63	>50
C2c		-CHO	1.35 ± 0.64	1.20 ± 0.14	>50
C2d		-CH(OH)SO_3Na	1.10 ± 0.57	1.45 ± 0.21	>50
C3c	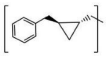	-CHO	0.69 ± 0.13	2.74 ± 2.14	>50
C3d		-CH(OH)SO_3Na	0.80 ± 0.14	4.02 ± 0.30	>50
C4c		-CHO	0.82 ± 0.15	2.74 ± 2.14	>50
C4d		-CH(OH)SO_3Na	1.35 ± 0.35	3.65 ± 0.63	>50
C5c		-CHO	1.05 ± 0.21	2.13 ± 0.49	>50
C5d		-CH(OH)SO_3Na	0.95 ± 0.22	1.89 ± 0.09	>50
C6c		-CHO	0.80 ± 0.05	3.30 ± 0.71	>50
C6d		-CH(OH)SO_3Na	0.58 ± 0.11	2.85 ± 0.49	>50
C7c		-CHO	0.59 ± 0.04	2.00 ± 0.14	>50
C7d		-CH(OH)SO_3Na	0.75 ± 0.07	2.15 ± 0.35	>50
C8c		-CHO	1.15 ± 0.08	NT[d]	>50
C8d		-CH(OH)SO_3Na	0.55 ± 0.07	NT	>50
C9c		-CHO	0.75 ± 0.14	2.95 ± 0.28	>50
C9d		-CH(OH)SO_3Na	0.84 ± 0.06	2.05 ± 0.64	>50
C10c		-CHO	1.25 ± 0.07	3.65 ± 1.48	>50
C10d		-CH(OH)SO_3Na	1.05 ± 0.21	2.85 ± 1.55	>50
C11c		-CHO	0.95 ± 0.21	1.08 ± 0.05	>50
C11d		-CH(OH)SO_3Na	0.45 ± 0.13	1.02 ± 0.17	>50
C12c		-CHO	0.50 ± 0.14	0.88 ± 0.25	>50
C12d		-CH(OH)SO_3Na	0.51 ± 0.06	1.25 ± 0.07	>50
C13c		-CHO	1.55 ± 0.07	2.95 ± 0.21	>50
C13d		-CH(OH)SO_3Na	0.75 ± 0.07	3.10 ± 0.42	>50
C14c		-CHO	0.63 ± 0.10	7.05 ± 0.78	>50
C14d		-CH(OH)SO_3Na	1.05 ± 0.64	6.30 ± 0.85	>50
C15c		-CHO	0.38 ± 0.11	0.45 ± 0.05	>50
C15d		-CH(OH)SO_3Na	0.29 ± 0.08	0.50 ± 0.11	>50
C16c		-CHO	0.36 ± 0.09	0.90 ± 0.06	>50
C16d		-CH(OH)SO_3Na	0.33 ± 0.04	1.21 ± 0.48	>50
C17c		-CHO	0.65 ± 0.07	>10	>50
C17d		-CH(OH)SO_3Na	0.75 ± 0.09	>10	>50

[a]IC_{50}, 50% inhibitory concentration.
[b]EC_{50}, 50% effective concentration; CC_{50}, 50% cytotoxic concentration (values are M ± SD).
[c]Mean (M) ± standard deviation (SD) of the means.
[d]NT, not tested.

Cytotoxicity assay

To determine the cytotoxicity of the compounds, 70%–80% confluent HEK293T cells in a 96-well plate were incubated with serial dilutions of each compound (up to 50 μM) for 24 h. Cell cytotoxicity was determined by a CytoTox 96 nonradioactive assay kit (Promega) by measuring cytosolic enzyme lactate dehydrogenase, following the manufacturer's

TABLE 3 The IC_{50}, EC_{50}, and CC_{50} values of compounds with a gem-dimethyl group (***D1c/d-D17c/d*** [47]) against FMDV 3Cpro in the enzyme and cell-based reporter assays

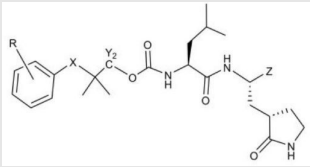

Com	R	X	Y	Z	FRET assay (IC_{50}, μM)[a]	Cell-based assay (EC_{50}, μM)[b]	CC_{50} (μM)
D1c	H	S	H	-CHO	1.20 ± 0.71[c]	1.85 ± 0.35	>50
D1d				-CH(OH)SO_3Na	1.01 ± 0.42	1.50 ± 0.43	>50
D1e					3.75 ± 0.07	5.00 ± 0.28	>50
D1f				-CN	>25	>10	>50
D2c	H	S	D	-CHO	1.52 ± 0.02	2.50 ± 0.42	>50
D2d				-CH(OH)SO_3Na	1.15 ± 0.07	2.91 ± 0.43	>50
D3c	H		H	-CHO	1.14 ± 0.08	>10	>50
D3d				-CH(OH)SO_3Na	1.05 ± 0.21	>10	>50
D4c	H		H	-CHO	0.90 ± 0.28	>10	>50
D4d				-CH(OH)SO_3Na	0.65 ± 0.09	>10	>50
D5c	m-F	S	H	-CHO	3.15 ± 0.49	1.00 ± 0.28	>50
D5d				-CH(OH)SO_3Na	0.81 ± 0.07	0.08 ± 0.14	>50
D6c	p-F	S	H	-CHO	0.91 ± 0.15	5.15 ± 0.64	>50
D6d				-CH(OH)SO_3Na	0.98 ± 0.11	5.85 ± 0.35	>50
D7c	m-Cl	S	H	-CHO	1.50 ± 0.28	1.05 ± 0.21	>50
D7d				-CH(OH)SO_3Na	0.60 ± 0.01	1.20 ± 0.14	>50
D8c	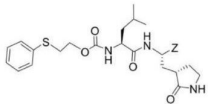			-CHO	1.35 ± 0.35	1.75 ± 0.21	>50
D8d				-CH(OH)SO_3Na	1.03 ± 0.24	1.95 ± 0.22	>50
D9c	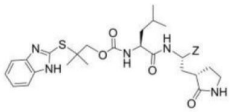			-CHO	2.15 ± 0.34	>10	>50
D9d				-CH(OH)SO_3Na	1.75 ± 0.92	>10	>50
D10c	H	O	H	-CHO	0.74 ± 0.08	NT[d]	>50
D10d				-CH(OH)SO_3Na	0.70 ± 0.28	NT	>50
D11c	p-Cl	O	H	-CHO	0.69 ± 0.06	0.64 ± 0.15	>50
D11d				-CH(OH)SO_3Na	0.49 ± 0.05	0.98 ± 1.11	>50
D12c	p-Cl	O	D	-CHO	0.14 ± 0.02	0.35 ± 0.10	>50
D12d				-CH(OH)SO_3Na	0.19 ± 0.01	0.43 ± 0.31	>50
D13c	m-Cl	O	H	-CHO	0.67 ± 0.08	5.34 ± 1.19	>50
D13d				-CH(OH)SO_3Na	0.65 ± 0.21	7.70 ± 0.85	>50
D14c	m-Cl	O	D	-CHO	0.50 ± 0.14	3.38 ± 0.39	>50
D14d				-CH(OH)SO_3Na	0.65 ± 0.07	4.81 ± 3.06	>50
D15c	p-F	O	H	-CHO	0.45 ± 0.07	5.25 ± 0.64	>50
D15d				-CH(OH)SO_3Na	0.55 ± 0.07	5.90 ± 0.58	>50
D16c	m-F	O	H	-CHO	0.78 ± 0.03	4.90 ± 0.37	>50
D16d				-CH(OH)SO_3Na	0.69 ± 0.02	5.05 ± 0.21	>50

(*Continued on next page*)

TABLE 3 The IC_{50}, EC_{50}, and CC_{50} values of compounds with a gem-dimethyl group (***D1c/d-D17c/d*** [47]) against FMDV 3Cpro in the enzyme and cell-based reporter assays (*Continued*)

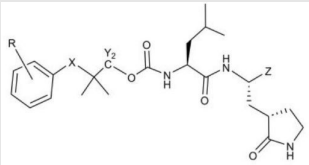

Com	R	X	Y	Z	FRET assay (IC_{50}, μM)[a]	Cell-based assay (EC_{50}, μM)[b]	CC_{50} (μM)
D17c	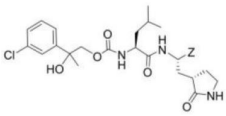			-CHO	2.00 ± 0.71	NT	>50
D17d				-CH(OH)SO_3Na	0.90 ± 0.28	NT	>50

[a]IC_{50}, 50% inhibitory concentration.
[b]EC_{50}, 50% effective concentration; CC_{50}, 50% cytotoxic concentration (values are mean ± SD).
[c]Mean (M) ± standard deviation (SD) of the means.
[d]NT, not tested.

instructions. The 50% cytotoxic concentration (CC_{50}) value of each compound was calculated using GraphPad Prism software. The non-specific cytotoxic effects of these compounds were also reported previously by us (35, 38, 40, 45, 47).

Three-dimensional modeling of FMDV 3Cpro bound with inhibitor *D12c*

The binding mode of ***D12c*** in the active site was modeled using the coordinates of a previously determined 3Cpro crystal structure of FMDV A serotype (Protein Data Bank accession no. 2BHG) by superimposing ***D12c*** in the active site of 3Cpro. The ***D12c***-bound 3Cpro model was prepared for docking by adding the covalent bond between ***D12c*** and the sulfur atom (Sg) of catalytic residue Cys163 and specifying His46 as the epsilon 2 nitrogen (HIE) tautomer with protonation of the nitrogen (Ne) atom. The protein preparation wizard in Schrodinger was used to optimize hydrogen bonding and minimize the structure, using Schrodinger's OSPL4 energy function (50), and ***D12c*** was prepared for docking using LigPrep (50). These models were subsequently used for covalent docking using CovDock, also from Schrödinger (50, 51), selecting the "Nucleophilic Addition to a Double Bond" reaction, performing MM-GBSA scoring with flexibility within 6 Å, and outputting five poses per ligand reaction site.

RESULTS

Multiple amino acid alignment of 3Cpro of various FMDV serotypes

The homology of 3Cpro amino acid sequences of the reference strains of FMDV serotypes was 84.51%–100% with conserved active site residues (His46, Asp84, and Cys163) (Fig. 2). FMDV serotypes A, O, and C and Asia1 share high 3Cpro homology at greater than 96% and a relatively lower homology with serotypes SAT1-3 at 85.45%–86.85%. The 3Cpro sequences are highly conserved with greater than 98% homology among SAT1–3 serotypes.

Activity of compounds against FMDV 3Cpro in the FRET assay

Aldehyde compound GC373 and its α-ketoamide or heterocycle dipeptidyl derivatives, which were previously reported to have activity against norovirus 3CLpro (45), inhibited FMDV 3Cpro with IC_{50} values >1 μM (Table 1). All dipeptidyl compounds with an α-ketoamide or α-heterocycle warhead had IC_{50} values comparable to GC373, ranging from 1.5 to 3.9 μM. Tripeptidyl compounds ***E1*** (**NPI52**) and ***E6*** showed strong inhibitory activity with 0.05 and 0.06 μM IC_{50} values, respectively (Table 1). AG7088, a tripeptidyl inhibitor of human rhinovirus 3Cpro, was less potent than tripeptidyl compounds ***E1*** (***NPI52***) and ***E6*** and most tested dipeptidyl compounds. The anti-FMDV

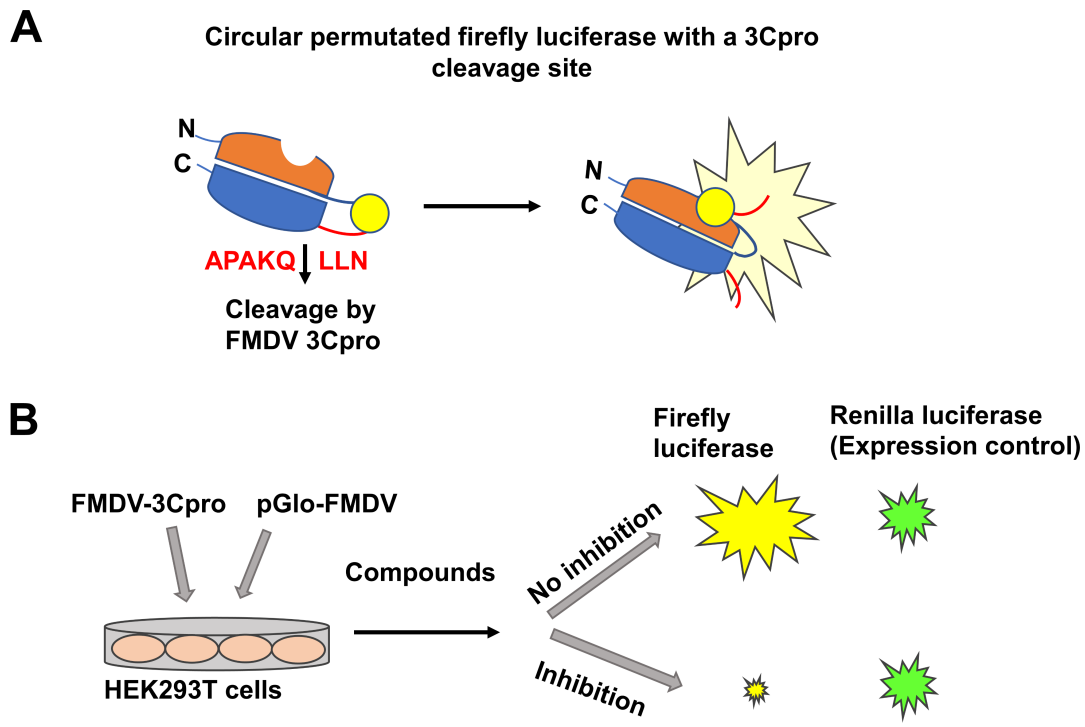

FIG 1 A cell-based reporter assay for screening FMDV 3Cpro inhibitors in HEK293T cells. (A) A plasmid encoding the permutated firefly luciferase with an FMDV 3Cpro cleavage sequence (pGlo-FMDV). The pGlo-FMDV plasmid also contains Renilla luciferase gene as an expression control. Cleavage of pGlo-FMDV by FMDV 3Cpro results in firefly luminescence. (B) Trypsinized HEK293T cells were electroporated with plasmids encoding FMDV 3Cpro and pGlo-FMDV and subsequently incubated with various concentrations of each compound. Following overnight incubation of the cells, luminescence was measured, and firefly luminescence was normalized against Renilla luminescence to determine the 50% effective concentration of each compound.

3Cpro activity of cyclopropane-based compounds (40) and gem-dimethyl compounds, which were recently reported to be potent coronavirus (SARS-CoV-2 and MERS-CoV) 3CLpro inhibitors (47), was also determined (Tables 2 and 3). All tested cyclopropane-based inhibitors in Table 2 showed good inhibitory activities (IC_{50} values of 0.29–1.55 μM) against FMDV 3Cpro. As expected, the aldehyde and bisulfite adduct pairs showed similar activities. Among cyclopropane-based inhibitors, ***C15c/C15d*** pair was most potent with IC_{50} values of 0.38 and 0.29 μM, respectively (Table 2). The potency of compounds with a gem-dimethyl group ranged from 0.14 to 3.75 μM, and among them, the ***D12c/D12d*** pair was most potent with IC_{50} values of 0.14 and 0.19 μM, respectively (Table 3). The dose-dependent inhibition curves of ***C15c*** and ***D12c*** in the FRET assay are shown in Fig. 3A.

Activity of compounds against FMDV 3Cpro in the cell-based reporter assay

The EC_{50} values of selected compounds were determined in this assay (Tables 1 to 3). All dipeptidyl compounds with an α-ketoamide or α-heterocycle warhead had EC_{50} values comparable to GC373 and ranged from 5.8 to 9.2 μM (Table 1). When a tripeptidyl compound with aldehyde (***E1***) or a ketoamide warhead (***E6***) (Table 1) was tested, they displayed good inhibitory activity with EC_{50} values of 0.11 and 0.15 μM, respectively (Table 1). The EC_{50} value of AG7088 was determined to be 10.3 μM. The EC_{50} values of the compounds in Tables 2 and 3 ranged from 0.35 to 7.7 μM. Among the tested dipeptidyl compounds in this assay system, ***D12c*** exhibited the highest potency with an EC_{50} value of 0.35 μM, which is consistent with the result from the FRET assay. The dose-dependent inhibition curves for ***C15c*** and ***D12c*** from the cell-based report assay are shown in Fig. 3B. All the compounds that were included in the study showed minimal cytotoxicity at up to 50 μM in HEK-293T cells (Tables 1–3).

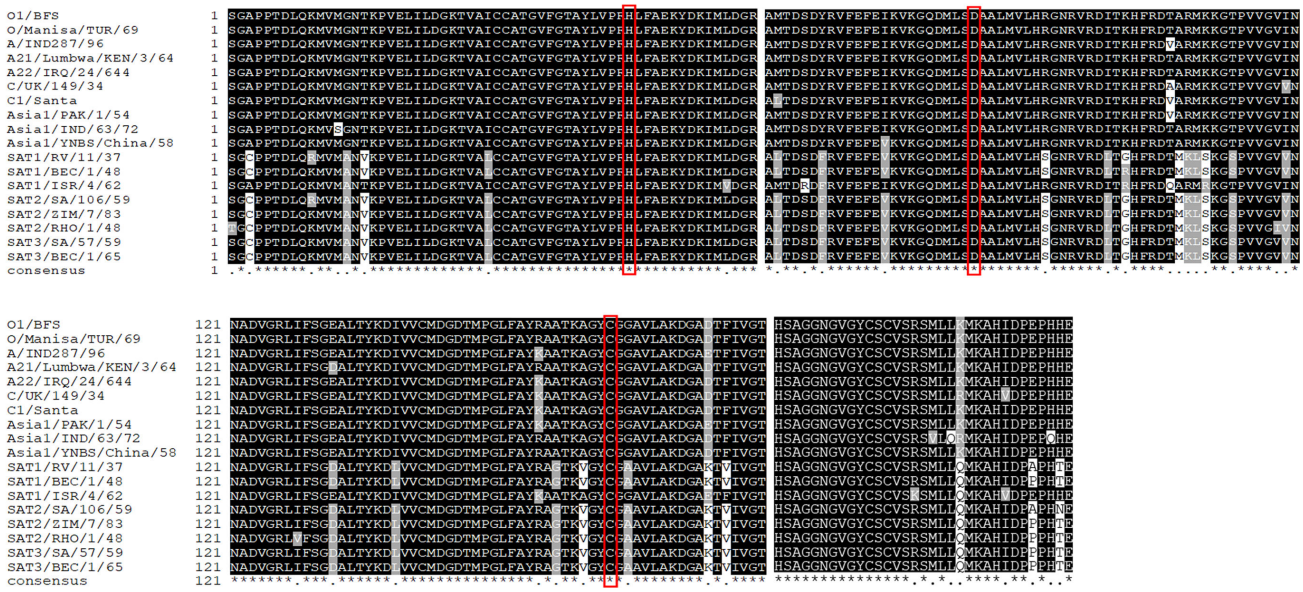

FIG 2 Multiple alignment of 3Cpro amino acid sequences of 18 FMDV prototype strains belonging to seven serotypes (O, A, C, Asia1, and SAT1–3). The conserved catalytic residues in the active site of 3Cpro are shown in red boxes.

Modelling of the binding mode of *D12c* to FMDV 3Cpro

The top 2 poses of the ***D12c*** adopt similar conformations in the FMDV 3Cpro active site where hydrogen bond interactions are formed between H46, T158, S182, H181, S182, and G184 (Fig. 4A and B). The main difference between the two poses is in the orientation of the *p*-chlorophenyl ring. The *p*-chlorophenyl ring of one pose is positioned away from M143 (pose 1), whereas the other forms a hydrogen bond with the backbone N-atom of M143 (pose 2). For both poses, the *p*-chlorophenyl ring is positioned in a hydrophobic cleft as shown in Fig. 4C. Comparison with the crystal structure of FMDV 3Cpro (Protein Data Bank 2BHG) revealed some interesting differences. Superposition (47) of the ***D12c***-bound structure with the apo structure of FMDV 3Cpro is similar overall with a root mean square deviation between Ca atoms at 1.10 Å (182 residues). The main difference is observed in the loop spanning A133-L155, which is disordered in 2BHG but adopts a β-sheet fold in the ***D12c***-bound model, where the loop moves toward the inhibitor to form a hydrogen bond with the backbone nitrogen of M143 in pose 2 and also engages in hydrophobic interactions (Fig. 4D).

DISCUSSION

The FMD genome encodes a single large polyprotein, which is proteolytically cleaved at 10 out of 13 cleavage sites by 3Cpro into functional viral proteins. This virally encoded, indispensable protease is highly conserved structurally and functionally among FMDV serotypes, which makes it an attractive target for the development of antivirals to formulate an additional layer of mitigation strategy, which can complement and strengthen the existing control measures for FMD outbreaks. Although limited number of studies are available on virus- or host-targeting antiviral agents of FMDV (9, 16, 17, 20, 22, 23, 26, 27, 52–55), some studies showed that pegylated recombinant interferon and T-1105 (polymerase inhibitor) reduced or prevented viremia in FMDV-challenged pigs (22, 52) and GS-9620, an agonist of toll-like receptor 7, enhanced survival rate in FMDV-vaccinated and un-vaccinated mice (16). Compounds that are shown to have *in vitro* activity against FMDV with EC_{50} values of low micromolar to millimolar range

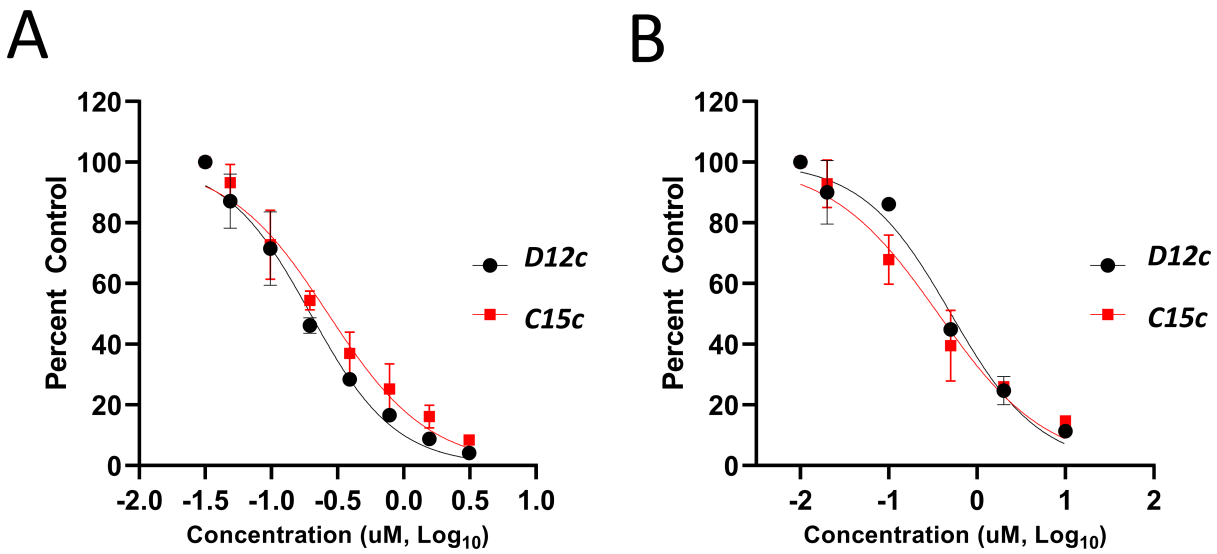

FIG 3 Dose-dependent inhibition curves of ***C15c*** and ***D12c*** from the FRET assay (A) and the cell-based reporter assay (B). Values are expressed as mean ± standard deviation of the means from at least three independent experiments.

include polymerase inhibitors 5D9 (20, 23), 24a (2-amino-4-arylthiazole derivatives) (24) and ribavirin (24), and a rhinovirus entry inhibitor pleconaril (17). These results, especially the *in vivo* data, support the potential use of antivirals in immediate emergency response as well as prophylactic treatment, but several issues, such as serotype/genotype-wide efficacy, pharmacokinetics, and potential combined use of different classes of antiviral agents, are needed to be addressed.

The overall designing of 3Cpro or 3CLpro inhibitors from our previous studies has primarily utilized a known peptidyl recognition element attached to various warheads, such as an aldehyde, α-keto heterocycle, or α-ketoamide, in the case of transition-state analog inhibitors, which interact with the active site Cys to yield a tetrahedral adduct (35, 53, 56–58). The warhead can also be a Michael acceptor, such as an α,β-unsaturated ester or vinyl sulfone which, in contrast to aldehydes and α-ketoamides, reacts with the active site Cys to form a covalently bound enzyme inhibitor adduct (59–65). The most extensively studied inhibitors of this class (Michael acceptors) are AG7088 and its variants, which have been shown to be active against various picornaviruses, including human rhinoviruses (59, 63, 66), enterovirus-D68 (61), and FMDV (25). The *in vitro* potency of AG7088 against FMDV was above 10–20 μM EC_{50} (25) and is comparable to the EC_{50} value obtained from the cell-based reporter assay reported herein.

We previously reported that compounds with an α-ketoamide warhead are slightly less active against calicivirus or coronavirus 3CLpros compared to their aldehyde counterparts (35, 45, 47, 67). We have also shown that compounds with an α-ketoamide warhead is highly effective against picornavirus 3Cpro and comparable to aldehyde counterparts (46). When the di- and tripeptidyl compounds with various ketoamide residues were evaluated to assess the effects of α-ketoamide warhead on FMDV 3Cpro, both compound series showed similar potency with α-ketoamide or aldehyde warheads (Table 1), which was similar to what we observed with picornavirus 3Cpros. Among the compound series evaluated in this study, the most potent compounds against FMDV 3Cpro were ***E1*** (***NPI52***) and ***E6*** with EC_{50} values 0.11 and 0.15 μM, respectively (Table 1). For these tripeptidyl compounds including ***E1*** and ***E6***, we previously reported that they are highly effective against calicivirus and coronavirus 3CLpros (34, 38), but they might not have favorable *in vivo* pharmacokinetics (34).

The cyclopropane-based inhibitors (Table 2) were recently reported by us (40) as highly potent inhibitors against 3CLpros of SARS-CoV-2, SARS-CoV, and MERS-CoV. In this study, it was shown that the cyclopropane-based inhibitors also have activity against

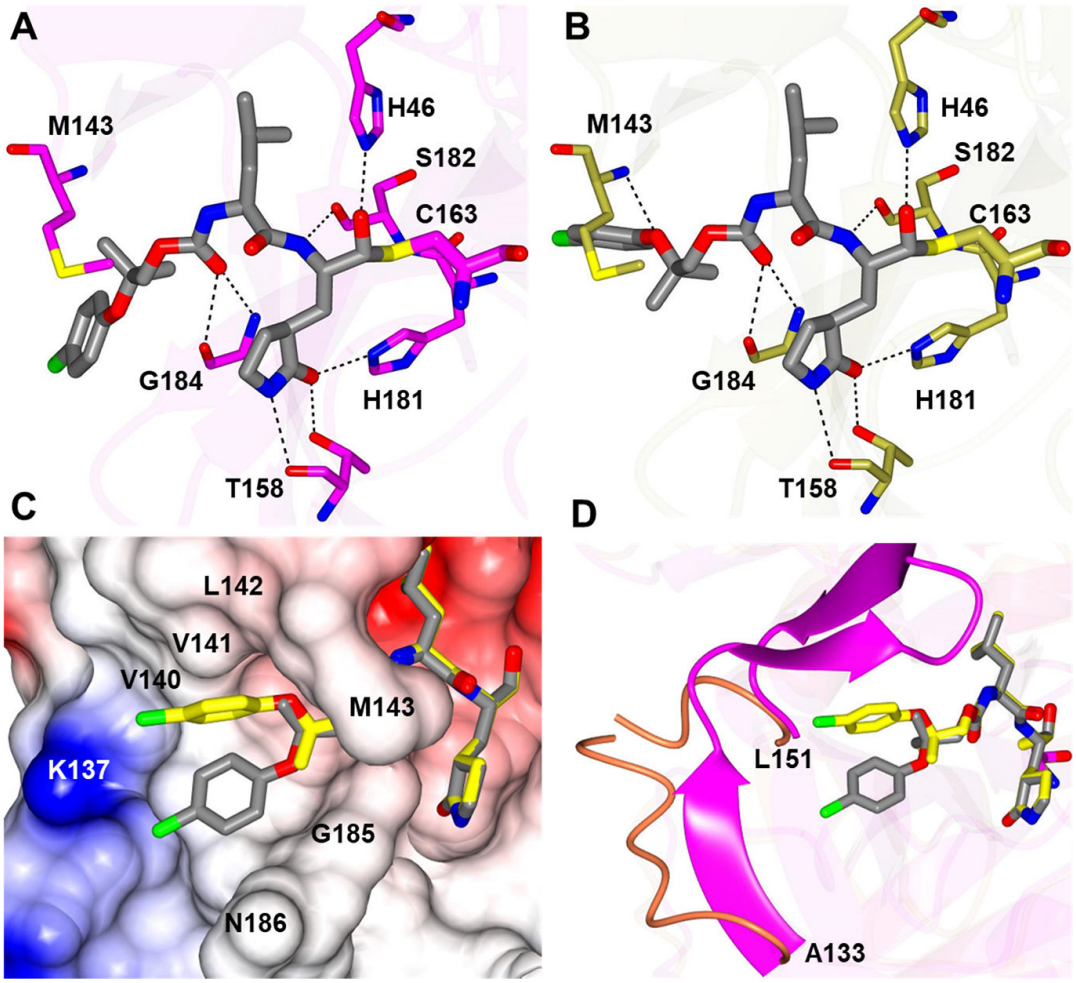

FIG 4 Modeling of ***D12c*** in the active site of FMDV 3Cpro. (A and B) Hydrogen bond interactions (dashed lines) for poses 1 and 2, respectively. (C) Electrostatic surface representation showing the putative orientation of *p*-chlorophenyl ring in the S4 subsite. (D) Superposition of ***D12c*** and the crystal structure of FMDV 3Cpro (Protein Data Bank 2BHG, magenta) highlights the differences in the loop spanning A133-L151. The poses 1 and 2 of ***D12c*** are colored gray and yellow, respectively.

FMDV 3Cpro with varying potency. Structure-activity relationship analysis of the series revealed that replacement of the methylene group in the cyclopropane ring with a gem-difluoro group did not increase potency (***C1c/d*** vs ***C2c/d***) (Table 2). Among the halogen substituted compounds, potency was also invariant to the nature and position of halogen substitution in the phenyl ring (compounds ***C5c/d*** through ***C8c/d***), and these compounds were also similar to the corresponding unsubstituted compound (***C1c/d***) in potency (Table 2). Furthermore, the isomeric methoxy-substituted phenyl compounds (***C9c/d, C10c/d***, and ***C11c/d***) were fairly effective against FMDV 3Cpro in the FRET assay (Table 2). However, replacement of the benzene ring with the cyclohexane ring increased potency by approximately twofold (***C1c/d*** vs ***C15c/d***). Among this series of inhibitors, ***C15c/C15d*** were most potent against FMDV 3Cpro with IC_{50} and EC_{50} values of 0.29–0.38 µM and 0.45–0.50 µM, respectively (Table 2). Compounds ***C15c/C15d*** also have activity against SARS-CoV-2 replicon in cell culture, but the most potent pairs against SARS-CoV-2 were ***C5c/d*** and ***C11c/d*** (EC_{50} 0.01–0.03 µM) (40), which suggests some differences in structural requirements for potency between these two viruses.

The second series of inhibitors (47) exploited the directional effects associated with the presence of a *gem*-dimethyl group that allowed the inhibitors to optimally interact with the S4 subsite of 3Cpro. The EC_{50} values of aldehyde ***D1c*** and its corresponding

bisulfite adduct ***D1d*** against SARS-CoV-2 were 0.012 and 0.010 μM, respectively (47). Previously, we reported that replacement of sulfur by oxygen (Table 3, X position) had varying effects in potency against 3CLpros of SARS-CoV-2 (decreased potency) and MERS-CoV (increased potency) (47). In the case of FMDV 3Cpro, replacement of sulfur by oxygen yielded more potent compounds (Table 3, ***D1c/d*** vs ***D10c/d***; ***D5c/d*** vs ***D16c/d***; ***D6c/d*** vs ***D15c/d***; and ***D7c/d*** vs ***D13c/d***). Interestingly, replacement of the aldehyde warhead with an α-ketoamide made no difference in potency against FMDV 3Cpro (***D1c*** vs ***D1e***), while the same replacement reduced potency against SARS-CoV-2 3CLpro (47). In addition, replacement with a nitrile warhead (***D1f***) diminished activity against FMDV 3Cpro at up to 25 μM (Table 3). When non-deuterated and deuterated pairs were compared for potency, some pairs showed unchanged activity (Table 3, ***D1c/d*** vs ***D2c/d*** and ***D11c/d*** vs ***D12c/d***), while deuteration of ***D11c/d*** to ***D12c/d*** moderately increased potency by approximately twofold (Table 3), making the ***D12c/d*** pair the most potent one against FMDV 3Cpro.

Among the compounds in Tables 2 and 3, the most potent compounds against FMDV 3Cpro were ***D12c*** and ***D12d*** with IC_{50} values 0.14 and 0.19 μM, respectively (Table 3), which is comparable to those with ***E1*** and ***E6*** (Table 1). Generally, IC_{50} values were comparable to EC_{50} values for each compound; however, some compounds showed variations between IC_{50} and EC_{50} values, especially the gem dimethyl series (Table 3), with better potency in the enzyme assay compared to the cell-based assay. The variation might be due to the cell permeability and stability of each compound, which highlights the importance of a cell-based assay for evaluating antiviral activity.

Recently, two papers (26, 27) by Theerawatanasirikul et al. and a paper by Lee et al. (9) showed natural products (including quercetin, luteolin, and isoginkgetin) and compounds (NSC116640 and NSC332670) from a chemical library inhibited the replication of FMDV in cell culture via inhibiting 3Cpro, and the molecular docking studies suggested that these compounds fit in the active site and interact with key residues of FMDV 3Cpro. In this study, the binding mode of ***D12c*** in the active site of FMDV 3Cpro was modeled by superimposing the compound on a previously determined crystal structure of 3Cpro. The non-deuterated counterpart of ***D12c*** [compound ***11d*** in Fig. 8A–C in reference (47)] was previously co-crystalized with SARS-CoV-2 3CLpro to identify the structural determinants associated with the binding of the inhibitor to the active site of SARS-CoV-2 3CLpro. The modeling shows that the five-ring glutamine surrogate tightly sites at S1 position with three hydrogen bonds with H181 and T158 of FMDV 3Cpro. In addition, hydrogen bonds are predicted between ***D12c*** and H46 and S182 and G184 of FMDV 3Cpro, which may explain the high potency of the compound. For *p*-chlorophenyl ring of ***D12c***, the modeled structure of FMDV 3Cpro and the co-crystal structure of SARS-CoV-2 bound to the inhibitor (47) showed that the residue has a similar orientation in the S4 subsite of both enzymes.

Screening many antiviral compounds against FMDV replication can be challenging as it requires biosafety level (BSL)-3E or 3Ag facility, and Plum Island Animal Disease Center is the only research facility in the US that can conduct research involving live virus. Thus, we established the FRET and cell-based reporter assays which can be used in BSL-2 laboratories, which can facilitate the drug discovery process for FMDV. In summary, we conducted structure-activity relationship studies on multiple series of protease inhibitors for FMDV 3Cpro using the FRET and the cell-based reporter assays and identified potent compounds with double-digit or triple-digit nanomolar EC_{50} values. The homology modeling and docking study revealed an insight into the binding mechanism between a 3Cpro inhibitor and FMDV 3Cpro. The identified inhibitors of FMDV 3Cpro warrant conducting further multiparameter optimization studies to identify one or more lead candidates for drug development for prophylactic and treatment options in immediate emergency response.

ACKNOWLEDGMENTS

The authors would like to thank David George for technical assistance.

This work was generously supported by U.S. Department of Agriculture (USDA), The National Institute of Food and Agriculture (NIFA) (2019-67015-29864), and the National Institutes of Health (NIH) (grants R01 AI130092 and AI161085).

AUTHOR AFFILIATIONS

[1]Department of Diagnostic Medicine and Pathobiology, College of Veterinary Medicine, Kansas State University, Manhattan, Kansas, USA
[2]Department of Chemistry, Wichita State University, Wichita, Kansas, USA
[3]Computational Chemical Biology Core, The University of Kansas, Lawrence, Kansas, USA
[4]Protein Structure and X-ray Crystallography Laboratory, The University of Kansas, Lawrence, Kansas, USA

AUTHOR ORCIDs

Yunjeong Kim http://orcid.org/0000-0002-2977-4400
Kyeong-Ok Chang http://orcid.org/0000-0002-4435-3751

FUNDING

Funder	Grant(s)	Author(s)
USDA | National Institute of Food and Agriculture (NIFA)	2019-67015-29864	Yunjeong Kim
HHS | National Institutes of Health (NIH)	R01 AI130092, AI161085	Kyeong-Ok Chang

AUTHOR CONTRIBUTIONS

Yunjeong Kim, Conceptualization, Data curation, Formal analysis, Funding acquisition, Investigation, Methodology, Project administration, Resources, Supervision, Writing – original draft, Writing – review and editing | Emma Pool, Investigation | Eunji Kim, Investigation | Chamandi S. Dampalla, Investigation | Harry Nhat Nguyen, Investigation | David K. Johnson, Formal analysis, Investigation | Scott Lovell, Formal analysis, Investigation | William C. Groutas, Conceptualization, Resources, Supervision, Validation | Kyeong-Ok Chang, Conceptualization, Funding acquisition, Resources, Supervision, Writing – original draft, Writing – review and editing

DATA AVAILABILITY

The detailed chemical structures are shown in Tables 1 to 3, and the detailed information on the synthesis of listed chemicals was reported in references 38, 40, 45, 47.

REFERENCES

1. Brown E, Nelson N, Gubbins S, Colenutt C. 2022. Airborne transmission of foot-and-mouth disease virus: a review of past and present perspectives. Viruses 14:1009. https://doi.org/10.3390/v14051009
2. Alexandersen S, Zhang Z, Donaldson AI, Garland AJM. 2003. The pathogenesis and diagnosis of Foot-and-Mouth disease. J Comp Pathol 129:1–36. https://doi.org/10.1016/s0021-9975(03)00041-0
3. Brito BP, Rodriguez LL, Hammond JM, Pinto J, Perez AM. 2017. Review of the global distribution of Foot-and-Mouth disease virus from 2007 to 2014. Transbound Emerg Dis 64:316–332. https://doi.org/10.1111/tbed.12373
4. Carriquiry M, Elobeid A, Hayes D. 2023. National impacts of a domestic outbreak of foot and mouth disease and African swine fever in the United States. Available from: https://www.card.iastate.edu/products/publications/pdf/23wp650.pdf
5. Pendell DL, Marsh TL, Coble KH, Lusk JL, Szmania SC. 2015. Economic assessment of FMDv releases from the national bio and agro defense facility. PLoS One 10:e0129134. https://doi.org/10.1371/journal.pone.0129134
6. United States Department of Agriculture (USDA). 2015. Foot-and-mouth disease (FMD) response ready reference guide - overview of emergency vaccination. Available from: https://www.aphis.usda.gov/animal_health/emergency_management/downloads/fmd_rrg_vaccination_plan.pdf
7. National Agriculture and Food Research Organization (NARO), National Institute of Animal Health (NIAH). 2022. FMD – Prevention and Preparedness in Japan. https://rr-asia.woah.org/wp-content/uploads/2022/10/17-japan_kazukimorioka_rev.pdf.
8. Australia's National Science Agency. 2023. Finding solutions to FMD. Available from: https://www.csiro.au/en/research/animals/livestock/foot-and-mouth-disease
9. Lee G, Kang HR, Kim A, Park JH, Lee MJ, Kim SM. 2023. Preventive effects of quercetin against Foot-and-Mouth disease virus *in vitro* and *in vivo* by inducing type I interferon. Front Microbiol 14:1121830. https://doi.org/10.3389/fmicb.2023.1121830
10. Kim SM, Park JH, Lee KN, Kim SK, Ko YJ, Lee HS, Cho IS. 2012. Enhanced inhibition of Foot-and-Mouth disease virus by combinations of porcine interferon-α and antiviral agents. Antiviral Res 96:213–220. https://doi.org/10.1016/j.antiviral.2012.09.009

11. Goris N, Vandenbussche F, De Clercq K. 2008. Potential of antiviral therapy and prophylaxis for controlling RNA viral infections of livestock. Antiviral Res 78:170–178. https://doi.org/10.1016/j.antiviral.2007.10.003
12. Kleina LG, Grubman MJ. 1992. Antiviral effects of a thiol protease inhibitor on Foot-and-Mouth-disease virus. J Virol 66:7168–7175. https://doi.org/10.1128/JVI.66.12.7168-7175.1992
13. Furuta Y, Takahashi K, Shiraki K, Sakamoto K, Smee DF, Barnard DL, Gowen BB, Julander JG, Morrey JD. 2009. T-705 (favipiravir) and related compounds: novel broad-spectrum inhibitors of RNA viral infections. Antiviral Res 82:95–102. https://doi.org/10.1016/j.antiviral.2009.02.198
14. Li D. 2010. Chitosan can stop or postpone the death of the suckling mice challenged with Foot-and-Mouth disease virus. Virol J 7:125. https://doi.org/10.1186/1743-422X-7-125
15. De Vleeschauwer AR, Lefebvre DJ, Willems T, Paul G, Billiet A, Murao LE, Neyts J, Goris N, De Clercq K. 2016. A refined guinea pig model of Foot-and-Mouth disease virus infection for assessing the efficacy of antiviral compounds. Transbound Emerg Dis 63:e205–e212. https://doi.org/10.1111/tbed.12255
16. Lee G, Kang HR, Kim A, Park JH, Lee MJ, Kim SM. 2022. Antiviral effect of vesatolimod (GS-9620) against Foot-and-Mouth disease virus both *in vitro* and *in vivo*. Antiviral Res 205:105384. https://doi.org/10.1016/j.antiviral.2022.105384
17. Soumajit S, Tamil Selvan RP, Bhanuprakash V. 2019. *In vitro* antiviral efficacy of pleconaril and ribavirin on Foot-and-Mouth disease virus replication. Virusdisease 30:562–570. https://doi.org/10.1007/s13337-019-00559-w
18. Airaksinen A, Pariente N, Menéndez-Arias L, Domingo E. 2003. Curing of Foot-and-Mouth disease virus from persistently infected cells by ribavirin involves enhanced mutagenesis. Virology 311:339–349. https://doi.org/10.1016/s0042-6822(03)00144-2
19. Perales C, Agudo R, Tejero H, Manrubia SC, Domingo E. 2009. Potential benefits of sequential inhibitor-mutagen treatments of RNA virus infections. PLoS Pathog 5:e1000658. https://doi.org/10.1371/journal.ppat.1000658
20. Rai DK, Schafer EA, Singh K, McIntosh MA, Sarafianos SG, Rieder E. 2013. Repeated exposure to 5D9, an inhibitor of 3D polymerase, effectively limits the replication of Foot-and-Mouth disease virus in host cells. Antiviral Res 98:380–385. https://doi.org/10.1016/j.antiviral.2013.03.022
21. Sahu TK, Gurjar AKS, Meher PK, Varghese C, Marwaha S, Rao GP, Rai A, Guleria N, Basagoudanavar SH, Sanyal A, Rao AR. 2020. Computational insights into RNAi-based therapeutics for foot and mouth disease of *Bos taurus*. Sci Rep 10:21593. https://doi.org/10.1038/s41598-020-78541-6
22. Nishi T, Fukai K, Masujin K, Kawaguchi R, Ikezawa M, Yamada M, Nakajima N, Komeno T, Furuta Y, Sugihara H, Kurosaki C, Sakamoto K, Morioka K. 2022. Administration of the antiviral agent T-1105 fully protects pigs from Foot-and-Mouth disease infection. Antiviral Res 208:105425. https://doi.org/10.1016/j.antiviral.2022.105425
23. Durk RC, Singh K, Cornelison CA, Rai DK, Matzek KB, Leslie MD, Schafer E, Marchand B, Adedeji A, Michailidis E, Dorst CA, Moran J, Pautler C, Rodriguez LL, McIntosh MA, Rieder E, Sarafianos SG. 2010. Inhibitors of foot and mouth disease virus targeting a novel pocket of the RNA-dependent RNA polymerase. PLoS One 5:e15049. https://doi.org/10.1371/journal.pone.0015049
24. Jeong KW, Lee JH, Park SM, Choi JH, Jeong DY, Choi DH, Nam Y, Park JH, Lee KN, Kim SM, Ku JM. 2015. Synthesis and *in-vitro* evaluation of 2-amino-4-arylthiazole as inhibitor of 3D polymerase against Foot-and-Mouth disease (FMD). Eur J Med Chem 102:387–397. https://doi.org/10.1016/j.ejmech.2015.08.020
25. van der Linden L, Ulferts R, Nabuurs SB, Kusov Y, Liu H, George S, Lacroix C, Goris N, Lefebvre D, Lanke KHW, De Clercq K, Hilgenfeld R, Neyts J, van Kuppeveld FJM. 2014. Application of a cell-based protease assay for testing inhibitors of picornavirus 3C proteases. Antiviral Res 103:17–24. https://doi.org/10.1016/j.antiviral.2013.12.012
26. Theerawatanasirikul S, Thangthamniyom N, Kuo CJ, Semkum P, Phecharat N, Chankeeree P, Lekcharoensuk P. 2021. Natural phytochemicals, luteolin and isoginkgetin, inhibit 3C protease and infection of FMDV, *in silico* and *in vitro*. Viruses 13:2118. https://doi.org/10.3390/v13112118
27. Theerawatanasirikul S, Lueangaramkul V, Pantanam A, Mana N, Semkum P, Lekcharoensuk P. 2023. Small molecules targeting 3C protease inhibit FMDV replication and exhibit virucidal effect in cell-based assays. Viruses 15:1887. https://doi.org/10.3390/v15091887
28. Dampalla C.S, Kim Y, Bickmeier N, Rathnayake AD, Nguyen HN, Zheng J, Kashipathy MM, Baird MA, Battaile KP, Lovell S, Perlman S, Chang KO, Groutas WC. 2021. Structure-guided design of conformationally constrained cyclohexane inhibitors of severe acute respiratory syndrome coronavirus-2 3CL protease. J Med Chem 64:10047–10058. https://doi.org/10.1021/acs.jmedchem.1c00319
29. Dampalla C.S, Rathnayake AD, Galasiti Kankanamalage AC, Kim Y, Perera KD, Nguyen HN, Miller MJ, Madden TK, Picard HR, Thurman HA, Kashipathy MM, Liu L, Battaile KP, Lovell S, Chang KO, Groutas WC. 2022. Structure-guided design of potent spirocyclic inhibitors of severe acute respiratory syndrome coronavirus-2 3C-like protease. J Med Chem 65:7818–7832. https://doi.org/10.1021/acs.jmedchem.2c00224
30. Dampalla CS, Rathnayake AD, Perera KD, Jesri A-R, Nguyen HN, Miller MJ, Thurman HA, Zheng J, Kashipathy MM, Battaile KP, Lovell S, Perlman S, Kim Y, Groutas WC, Chang K-O. 2021. Structure-guided design of potent inhibitors of SARS-CoV-2 3CL protease: structural, biochemical, and cell-based studies. J Med Chem 64:17846–17865. https://doi.org/10.1021/acs.jmedchem.1c01037
31. Dampalla CS, Zheng J, Perera KD, Wong L-Y, Meyerholz DK, Nguyen HN, Kashipathy MM, Battaile KP, Lovell S, Kim Y, Perlman S, Groutas WC, Chang K-O. 2021. Postinfection treatment with a protease inhibitor increases survival of mice with a fatal SARS-CoV-2 infection. Proc Natl Acad Sci U S A 118:e2101555118. https://doi.org/10.1073/pnas.2101555118
32. Galasiti Kankanamalage A.C, Kim Y, Rathnayake AD, Damalanka VC, Weerawarna PM, Doyle ST, Alsoudi AF, Dissanayake DMP, Lushington GH, Mehzabeen N, Battaile KP, Lovell S, Chang KO, Groutas WC. 2017. Structure-based exploration and exploitation of the S4 subsite of norovirus 3CL protease in the design of potent and permeable inhibitors. Eur J Med Chem 126:502–516. https://doi.org/10.1016/j.ejmech.2016.11.027
33. Galasiti Kankanamalage AC, Kim Y, Weerawarna PM, Uy RAZ, Damalanka VC, Mandadapu SR, Alliston KR, Mehzabeen N, Battaile KP, Lovell S, Chang K-O, Groutas WC. 2015. Structure-guided design and optimization of dipeptidyl inhibitors of norovirus 3CL protease. structure-activity relationships and biochemical, X-ray crystallographic, cell-based, and *in vivo* studies. J Med Chem 58:3144–3155. https://doi.org/10.1021/jm5019934
34. Kim Y, Liu H, Galasiti Kankanamalage AC, Weerasekara S, Hua DH, Groutas WC, Chang K-O, Pedersen NC, Perlman S. 2016. Reversal of the progression of fatal coronavirus infection in cats by a broad-spectrum coronavirus protease inhibitor. PLoS Pathog 12:e1005531. https://doi.org/10.1371/journal.ppat.1005531
35. Kim Y, Lovell S, Tiew K-C, Mandadapu SR, Alliston KR, Battaile KP, Groutas WC, Chang K-O. 2012. Broad-spectrum antivirals against 3C or 3C-like proteases of picornaviruses, noroviruses, and coronaviruses. J Virol 86:11754–11762. https://doi.org/10.1128/JVI.01348-12
36. Kim Y, Shivanna V, Narayanan S, Prior AM, Weerasekara S, Hua DH, Kankanamalage ACG, Groutas WC, Chang K-O. 2015. Broad-spectrum inhibitors against 3C-like proteases of feline coronaviruses and feline caliciviruses. J Virol 89:4942–4950. https://doi.org/10.1128/JVI.03688-14
37. Mandadapu SR, Gunnam MR, Tiew K-C, Uy RAZ, Prior AM, Alliston KR, Hua DH, Kim Y, Chang K-O, Groutas WC. 2013. Inhibition of norovirus 3CL protease by bisulfite adducts of transition state inhibitors. Bioorg Med Chem Lett 23:62–65. https://doi.org/10.1016/j.bmcl.2012.11.026
38. Prior AM, Kim Y, Weerasekara S, Moroze M, Alliston KR, Uy RAZ, Groutas WC, Chang KO, Hua DH. 2013. Design, synthesis, and bioevaluation of viral 3C and 3C-like protease inhibitors. Bioorg Med Chem Lett 23:6317–6320. https://doi.org/10.1016/j.bmcl.2013.09.070
39. Rathnayake AD, Zheng J, Kim Y, Perera KD, Mackin S, Meyerholz DK, Kashipathy MM, Battaile KP, Lovell S, Perlman S, Groutas WC, Chang KO. 2020. 3C-like protease inhibitors block coronavirus replication *in vitro* and improve survival in MERS-CoV-infected mice. Sci Transl Med 12:eabc5332. https://doi.org/10.1126/scitranslmed.abc5332
40. Dampalla CS, Nguyen HN, Rathnayake AD, Kim Y, Perera KD, Madden TK, Thurman HA, Machen AJ, Kashipathy MM, Liu L, Battaile KP, Lovell S, Chang K-O, Groutas WC. 2023. Broad-spectrum cyclopropane-based inhibitors of coronavirus 3C-like proteases: biochemical, structural, and virological studies. ACS Pharmacol Transl Sci 6:181–194. https://doi.org/10.1021/acsptsci.2c00206

41. Galasiti Kankanamalage AC, Kim Y, Damalanka VC, Rathnayake AD, Fehr AR, Mehzabeen N, Battaile KP, Lovell S, Lushington GH, Perlman S, Chang K-O, Groutas WC. 2018. Structure-guided design of potent and permeable inhibitors of MERS coronavirus 3CL protease that utilize a piperidine moiety as a novel design element. Eur J Med Chem 150:334–346. https://doi.org/10.1016/j.ejmech.2018.03.004
42. Perera KD, Johnson DK, Lovell S, Groutas WC, Chang KO, Kim Y. 2022. Potent protease inhibitors of highly pathogenic lagoviruses: rabbit hemorrhagic disease virus and european brown hare syndrome virus. Microbiol Spectr 10. https://doi.org/10.1128/spectrum.00142-22
43. Li P, Kim Y, Dampalla CS, Nguyen HN, Meyerholz DK, Johnson DK, Lovell S, Groutas WC, Perlman S, Chang KO. 2023. Potent 3CLpro inhibitors effective against SARS-CoV-2 and MERS-CoV in animal models by therapeutic treatment. mBio. https://doi.org/10.1128/mbio.02878-23
44. Mandadapu SR, Weerawarna PM, Prior AM, Uy RAZ, Aravapalli S, Alliston KR, Lushington GH, Kim Y, Hua DH, Chang K-O, Groutas WC. 2013. Macrocyclic inhibitors of 3C and 3C-like proteases of picornavirus, norovirus, and coronavirus. Bioorg Med Chem Lett 23:3709–3712. https://doi.org/10.1016/j.bmcl.2013.05.021
45. Mandadapu SR, Weerawarna PM, Gunnam MR, Alliston KR, Lushington GH, Kim Y, Chang K-O, Groutas WC. 2012. Potent inhibition of norovirus 3CL protease by peptidyl α-ketoamides and α-ketoheterocycles. Bioorg Med Chem Lett 22:4820–4826. https://doi.org/10.1016/j.bmcl.2012.05.055
46. Kim Y, Kankanamalage ACG, Damalanka VC, Weerawarna PM, Groutas WC, Chang K-O. 2016. Potent inhibition of enterovirus D68 and human rhinoviruses by dipeptidyl aldehydes and α-ketoamides. Antiviral Res 125:84–91. https://doi.org/10.1016/j.antiviral.2015.11.010
47. Dampalla CS, Miller MJ, Kim Y, Zabiegala A, Nguyen HN, Madden TK, Thurman HA, Machen AJ, Cooper A, Liu L, Battaile KP, Lovell S, Chang KO, Groutas WC. 2023. Structure-guided design of direct-acting antivirals that exploit the gem-dimethyl effect and potently inhibit 3CL proteases of severe acute respiratory syndrome coronavirus-2 (SARS-CoV-2) and middle east respiratory syndrome coronavirus (MERS-CoV). Eur J Med Chem 254:115376. https://doi.org/10.1016/j.ejmech.2023.115376
48. Perera KD, Galasiti Kankanamalage AC, Rathnayake AD, Honeyfield A, Groutas W, Chang KO, Kim Y. 2018. Protease inhibitors broadly effective against feline, ferret and mink coronaviruses. Antiviral Res 160:79–86. https://doi.org/10.1016/j.antiviral.2018.10.015
49. Galbán S, Jeon YH, Bowman BM, Stevenson J, Sebolt KA, Sharkey LM, Lafferty M, Hoff BA, Butler BL, Wigdal SS, Binkowski BF, Otto P, Zimmerman K, Vidugiris G, Encell LP, Fan F, Wood KV, Galbán CJ, Ross BD, Rehemtulla A. 2013. Imaging proteolytic activity in live cells and animal models. PLoS One 8:e66248. https://doi.org/10.1371/journal.pone.0066248
50. Schrödinger LLC. 2019. Schrödinger release 2019-4: protein preparation wizard; Epik; Impact; Prime; Glide; LigPrep; induced fit docking protocol. CovDock, New York, NY.
51. Zhu K, Shirts MR, Friesner RA. 2007. Improved methods for side chain and loop predictions via the protein local optimization program: variable dielectric model for implicitly improving the treatment of polarization effects. J Chem Theory Comput 3:2108–2119. https://doi.org/10.1021/ct700166f
52. Diaz-San Segundo F, Medina GN, Azzinaro P, Gutkoska J, Mogulothu A, Attreed SE, Lombardi KR, Shields J, Hudock TA, de los Santos T. 2021. Use of protein pegylation to prolong the antiviral effect of IFN against FMDV. Front Microbiol 12:668890. https://doi.org/10.3389/fmicb.2021.668890
53. Ramajayam R, Tan KP, Liang PH. 2011. Recent development of 3C and 3CL protease inhibitors for anti-coronavirus and anti-picornavirus drug discovery. Biochem Soc Trans 39:1371–1375. https://doi.org/10.1042/BST0391371
54. Li SF, Gong MJ, Sun YF, Shao JJ, Zhang YG, Chang HY. 2019. Antiviral activity of brequinar against Foot-and-Mouth disease virus infection *in vitro* and *in vivo*. Biomed Pharmacother 116:108982. https://doi.org/10.1016/j.biopha.2019.108982
55. Li SF, Gong MJ, Sun YF, Shao JJ, Zhang YG, Chang HY. 2019. *In vitro* and *in vivo* antiviral activity of mizoribine against Foot-and-Mouth disease virus. Molecules 24:1723. https://doi.org/10.3390/molecules24091723
56. Zhai Y, Ma Y, Ma F, Nie Q, Ren X, Wang Y, Shang L, Yin Z. 2016. Structure-activity relationship study of peptidomimetic aldehydes as enterovirus 71 3C protease inhibitors. Eur J Med Chem 124:559–573. https://doi.org/10.1016/j.ejmech.2016.08.064
57. Zhang L, Lin D, Kusov Y, Nian Y, Ma Q, Wang J, von Brunn A, Leyssen P, Lanko K, Neyts J, de Wilde A, Snijder EJ, Liu H, Hilgenfeld R. 2020. α-ketoamides as broad-spectrum inhibitors of coronavirus and enterovirus replication: structure-based design, synthesis, and activity assessment. J Med Chem 63:4562–4578. https://doi.org/10.1021/acs.jmedchem.9b01828
58. Ma Y, Shang C, Yang P, Li L, Zhai Y, Yin Z, Wang B, Shang L. 2018. 4-iminooxazolidin-2-one as a bioisostere of the cyanohydrin moiety: inhibitors of enterovirus 71 3C protease. J Med Chem 61:10333–10339. https://doi.org/10.1021/acs.jmedchem.8b01335
59. Patick AK, Binford SL, Brothers MA, Jackson RL, Ford CE, Diem MD, Maldonado F, Dragovich PS, Zhou R, Prins TJ, Fuhrman SA, Meador JW, Zalman LS, Matthews DA, Worland ST. 1999. *In vitro* antiviral activity of AG7088, a potent inhibitor of human rhinovirus 3C protease. Antimicrob Agents Chemother 43:2444–2450. https://doi.org/10.1128/AAC.43.10.2444
60. Dragovich PS, Prins TJ, Zhou R, Webber SE, Marakovits JT, Fuhrman SA, Patick AK, Matthews DA, Lee CA, Ford CE, Burke BJ, Rejto PA, Hendrickson TF, Tuntland T, Brown EL, Meador JW, Ferre RA, Harr JE, Kosa MB, Worland ST. 1999. Structure-based design, synthesis, and biological evaluation of irreversible human rhinovirus 3C protease inhibitors. 4. incorporation of P1 lactam moieties as L-glutamine replacements. J Med Chem 42:1213–1224. https://doi.org/10.1021/jm9805384
61. Tan J, George S, Kusov Y, Perbandt M, Anemüller S, Mesters JR, Norder H, Coutard B, Lacroix C, Leyssen P, Neyts J, Hilgenfeld R. 2013. 3C protease of enterovirus 68: structure-based design of Michael acceptor inhibitors and their broad-spectrum antiviral effects against picornaviruses. J Virol 87:4339–4351. https://doi.org/10.1128/JVI.01123-12
62. Kuo C-J, Shie J-J, Fang J-M, Yen G-R, Hsu JT-A, Liu H-G, Tseng S-N, Chang S-C, Lee C-Y, Shih S-R, Liang P-H. 2008. Design, synthesis, and evaluation of 3C protease inhibitors as anti-enterovirus 71 agents. Bioorg Med Chem 16:7388–7398. https://doi.org/10.1016/j.bmc.2008.06.015
63. Matthews DA, Dragovich PS, Webber SE, Fuhrman SA, Patick AK, Zalman LS, Hendrickson TF, Love RA, Prins TJ, Marakovits JT, Zhou R, Tikhe J, Ford CE, Meador JW, Ferre RA, Brown EL, Binford SL, Brothers MA, DeLisle DM, Worland ST. 1999. Structure-assisted design of mechanism-based irreversible inhibitors of human rhinovirus 3C protease with potent antiviral activity against multiple rhinovirus serotypes. Proc Natl Acad Sci U S A 96:11000–11007. https://doi.org/10.1073/pnas.96.20.11000
64. Ma Y, Li L, He S, Shang C, Sun Y, Liu N, Meek TD, Wang Y, Shang L. 2019. Application of dually activated Michael acceptor to the rational design of reversible covalent inhibitor for enterovirus 71 3C protease. J Med Chem 62:6146–6162. https://doi.org/10.1021/acs.jmedchem.9b00387
65. Schulz R, Atef A, Becker D, Gottschalk F, Tauber C, Wagner S, Arkona C, Abdel-Hafez AA, Farag HH, Rademann J, Wolber G. 2018. Phenylthiomethyl ketone-based fragments show selective and irreversible inhibition of enteroviral 3C proteases. J Med Chem 61:1218–1230. https://doi.org/10.1021/acs.jmedchem.7b01440
66. Hung H-C, Wang H-C, Shih S-R, Teng I-F, Tseng C-P, Hsu JT-A. 2011. Synergistic inhibition of enterovirus 71 replication by interferon and rupintrivir. J Infect Dis 203:1784–1790. https://doi.org/10.1093/infdis/jir174
67. Tiew K-C, He G, Aravapalli S, Mandadapu SR, Gunnam MR, Alliston KR, Lushington GH, Kim Y, Chang K-O, Groutas WC. 2011. Design, synthesis, and evaluation of inhibitors of Norwalk virus 3C protease. Bioorg Med Chem Lett 21:5315–5319. https://doi.org/10.1016/j.bmcl.2011.07.016